RAL-TR-1999-043
TSL/ISV-99-0217
TIFR/TH/99-49
September 1999

Detecting heavy charged Higgs bosons at the LHC with triple b-tagging

S. Moretti[1,2] and D.P. Roy[3]

[1] *Rutherford Appleton Laboratory, Chilton, Didcot, Oxon OX11 0QX, UK*
[2] *Dept. of Radiation Sciences, Uppsala University, P.O. Box 535, 75121 Uppsala, Sweden*
[3] *Tata Institute of Fundamental Research, Mumbai - 400 005, India*

Abstract

We investigate the charged Higgs boson signal at the LHC using its dominant production and decay modes with triple b-tagging, i.e. $tH^- \to t\bar{t}b \to b\bar{b}bW^+W^-$, followed by leptonic decay of one W and hadronic decay of the other. We consider the continuum background from the associated production of $t\bar{t}$ with a b- or a light quark or gluon jet, which can be mis-tagged as b-jet. We reconstruct the top quark masses to identify the 3rd b-jet accompanying the $t\bar{t}$ pair, and use its p_T distribution to distinguish the signal from the background. Combining this with the reconstruction of the $H^\pm$ mass gives a viable signature over two interesting regions of the parameter space – i.e. $\tan\beta \sim 1$ and $\sim m_t/m_b$.

The Minimal Supersymmetric Standard Model (MSSM) contains two complex Higgs doublets, ϕ_1 and ϕ_2, corresponding to eight scalar states. Three of these are absorbed as Goldstone bosons leaving five physical states – the two neutral scalars (h^0, H^0), a pseudo-scalar (A^0) and a pair of charged Higgs bosons $(H^\pm)$. All the tree-level masses and couplings of these particles are given in terms of two parameters, $M_{H^\pm}$ and $\tan\beta$, the latter representing the ratio of the vacuum expectation values of ϕ_1 and ϕ_2 [1]. While any one of the above neutral Higgs bosons may be hard to distinguish from that of the Standard Model, the $H^\pm$ carries a distinctive signature of the Supersymmetric (SUSY) Higgs sector. Moreover the couplings of the $H^\pm$ are uniquely related to $\tan\beta$, since the physical charged Higgs boson corresponds to the combination

$$H^\pm = -\phi_1^\pm \sin\beta + \phi_2^\pm \cos\beta. \tag{1}$$

Therefore the detection of $H^\pm$ and measurement of its mass and couplings are expected to play a very important role in probing the SUSY Higgs sector.

Unfortunately it is very hard to extend the $H^\pm$ search beyond the top quark mass at the Large Hadron Collider (LHC), because in this case the combination of dominant production and decay channels, $tH^- \to t\bar{t}b$, suffers from a large QCD background. The viability of a $H^\pm$ signal in this channel had been investigated in [2,3] assuming triple b-tagging. Recently it was shown that with four b-tags one can get a better signal/background ratio, but at the cost of a smaller signal size [4]. Similar conclusions were also found for the $H^\pm$ signal in its τ decay channel [5]. The charged Higgs boson signal at the LHC has also been investigated recently in subdominant production channels, $H^\pm W^\mp$ [6] and $H^\pm H^\mp$ [7], as well as the subdominant decay mode $H^\pm \to W^\pm h^0$ [8]. But it turns out to be at best marginal in each of these cases.

It is clear from the above discussion that the largest size of the $H^\pm$ signal is expected to come from its dominant production and decay channels with triple b-tagging. The purpose of this paper is to reinvestigate the $H^\pm$ signal in this channel in the light of the theoretical and experimental developments since the last analyses [2,3]. Several distinctions of the present study in comparison with those earlier ones are worth mentioning here.

i) The signal cross-section was calculated in [2] and [3] using the $2 \to 2$ and $2 \to 3$ processes respectively, i.e.

$$gb \to tH^- + \text{h.c.}, \tag{2}$$

and

$$gg \to t\bar{b}H^- + \text{h.c.}, \tag{3}$$

followed by the $H^- \to \bar{t}b$ decay. Here we shall instead combine the two cross-sections and subtract out the overlapping piece to avoid double counting, as suggested in [9,10].

ii) We shall use the p_T distribution of the 3rd b-tagged jet, accompanying the $t\bar{t}$ pair, for a better separation of the signal from the background.

iii) The actual value of top quark mass (175 GeV) will be used here instead of the illustrative values used in [2,3].

iv) Besides we shall be using current estimates of the b-tagging efficiency and rapidity coverage for the LHC [11] along with more recent structure functions [12,13].

The cross-section for the $2 \to 2$ process (2) is simple to calculate, while analytic expressions for the $2 \to 3$ processes (3) can be found in [4]. The resulting signal cross-sections shall be obtained by convoluting these partonic cross-sections with the MRS-LO(05A) parton densities [12]. We have also checked that essentially identical results are obtained with the CTEQ4L parton densities [13]. It may be noted here that both these cross-sections are controlled by the Yukawa coupling of the tbH vertex,

$$\frac{g}{\sqrt{2}M_W} H^+ \left[\cot\beta m_t \bar{t} b_L + \tan\beta m_b \bar{t} b_R\right] + \text{h.c.} \tag{4}$$

Consequently one gets fairly large values of the signal cross-section at the two ends of the MSSM allowed region,

$$\tan\beta \sim 1 \text{ and } \tan\beta \sim m_t/m_b, \tag{5}$$

with a pronounced minimum at $\tan\beta = \sqrt{m_t/m_b}$.

The question of overlap between the two $H^\pm$ production processes (2) and (3) has been recently discussed in [9,10]. The b-quark in (2) comes from a gluon in the proton beam splitting into a collinear $b\bar{b}$ pair, resulting in a large factor of $\alpha_S \log(Q/m_b)$, where the factorisation scale is

$$Q \simeq m_t + M_{H^\pm}. \tag{6}$$

This factor is then resummed to all orders, $\alpha_S^n \log^n(Q/m_b)$, in evaluating the phenomenological b-quark structure function [14,15]. The 1st order contribution to the structure function is given by the perturbative solution to the DGLAP equation,

$$b'(x,Q) = \frac{\alpha_S}{\pi} \log\left(\frac{Q}{m_b}\right) \int_x^1 \frac{dy}{y} P_{gb}\left(\frac{x}{y}\right) g(y,Q), \tag{7}$$

where $P_{gb}(z) = (z^2 + (1-z)^2)/2$ is the gluon splitting function. The resulting contribution to $gb \to tH^-$ is already accounted for by $gg \to t\bar{b}H^-$ in the collinear limit. Thus while combining (2) and (3), the above contribution should be subtracted from the former to avoid double counting.

Fig. 1 shows the cross-sections for (2) and (3) at the LHC energy (14 TeV) against the $H^\pm$ mass at $\tan\beta = 40$, using $m_b = 4.5$ GeV. It also shows their combined value, after subtracting out the gb' contribution from the former. While the cross-section for (2) is 2–3 times larger than that for (3), the bulk of the former is accounted for by the gb' contribution. Hence the combined cross-section is larger than that of (3) by only a factor of about 1.6. We also have checked that detection efficiencies for the processes (2) and (3) are very similar, since the extra b-jet in the latter case is relatively soft (missing the $p_T > 30$ selection cut discussed below over 70% of the time). We shall therefore simply multiply the cross-section for the $2 \to 3$ process (3) by the above mentioned factor of 1.6 in presenting the signal cross-sections.

It should also be mentioned here that the electroweak loop corrections to the tbH vertex (4) have been estimated to give up to 20% reduction in the signal cross-section depending

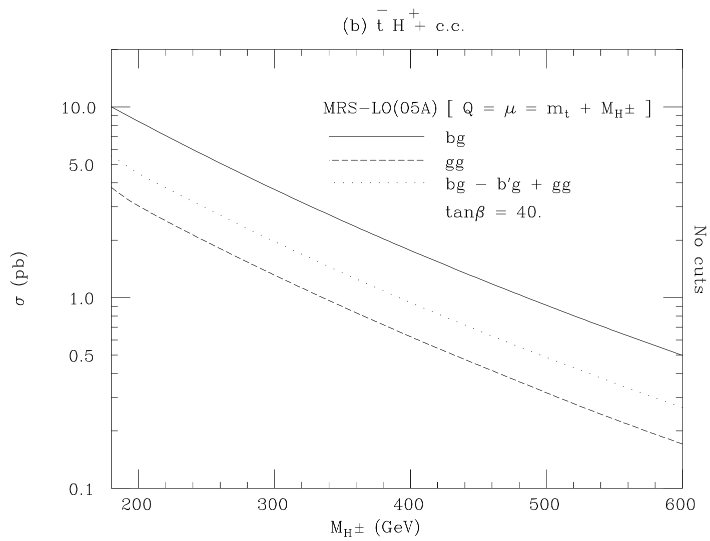

Figure 1: Cross section of the $2 \to 2$ process $gb \to tH^-$ (2), of the $2 \to 3$ one $gg \to t\bar{b}H^-$ (3) and of their sum after the subtraction of the gb' contribution, see eq. (7), for $\tan\beta = 40$ (including the charged conjugated final states). The PDF set used was MRS-LO(05A) with renormalisation and factorisation scales set equal to $m_t + M_{H^\pm}$. Normalisation is to the total cross sections without any branching ratios.

on $M_{H^\pm}$ and $\tan\beta$ [16]. The corresponding QCD corrections are expected to be larger, but not yet available. Note that higher-order QCD effects in the $H^- \to \bar{t}b$ decay are easily accounted for by using the running value of the b mass, $m_b(M_{H^\pm})$, in the tbH coupling. We shall therefore use it in estimating the $H^- \to \bar{t}b$ decay rate. (Of course this has no significant impact on the signal since this branching fraction amounts to $\gtrsim$80% over most of the parameter space of our interest.) The effects of SUSY QCD corrections may be larger, depending on the SUSY parameters [17]. We shall neglect this by assuming a large SUSY mass scale $\sim$ 1 TeV.

The final state resulting from the above $2 \to 2$ ($2 \to 3$) signal process is

$$tH^-(\bar{b}) \to t\bar{t}b(\bar{b}) \to b\bar{b}b(\bar{b})W^+W^-. \tag{8}$$

We shall require leptonic decay of one W and hadronic decay of the other, resulting in a final state of

$$b\bar{b}b(\bar{b})\ell\nu q\bar{q}. \tag{9}$$

The hard lepton (e, μ) will be required for triggering and suppression of multi-jet background, while the presence of only one ν will enable us to do mass reconstruction. As mentioned earlier, the extra b-quark coming from the $2 \to 3$ process (3) is expected to be too soft to pass our selection cuts or be tagged with a reasonable efficiency. We shall therefore require a minimum of 3 b-tagged and 2 untagged jets along with a lepton and a missing-p_T ($\not{p}_T$).

We shall consider the background to the final state (9) coming from

$$gb \to t\bar{t}b \to b\bar{b}bW^+W^-, \tag{10}$$

$$gg, q\bar{q} \to t\bar{t}g^\star \to b\bar{b}b\bar{b}W^+W^-, \tag{11}$$

along with those from

$$\begin{aligned} gg, q\bar{q} &\to t\bar{t}g \to b\bar{b}gW^+W^-, \\ gq &\to t\bar{t}q \to b\bar{b}qW^+W^-, \end{aligned} \tag{12}$$

where the gluon or light quark jet (j) is mis-tagged as a b-jet. In fact (12) will turn out to be the largest background. The cross-sections for processes (10)–(12) are computed using MadGraph and HELAS [18,19].

Our analysis is based on simply a parton level Monte Carlo program. However we have tried to simulate detector resolution by a Gaussian smearing of all jet momenta with [2]

$$(\sigma(p_T)/p_T)^2 = (0.6/\sqrt{p_T})^2 + (0.04)^2, \tag{13}$$

and the lepton momentum with

$$(\sigma(p_T)/p_T)^2 = (0.12/\sqrt{p_T})^2 + (0.01)^2. \tag{14}$$

The $\not{p}_T$ is obtained by vector addition of all the p_T's after resolution smearing.

As a basic set of selection cuts we require

$$p_T > 30 \text{ GeV} \quad \text{and} \quad |\eta| < 2.5 \tag{15}$$

for all the jets and the lepton, where η denotes pseudorapidity and the p_T-cut is applied to the $\not{p}_T$ as well. We also require a minimum separation of (ϕ is the azimuthal angle)

$$\Delta R = \left[(\Delta\phi)^2 + (\Delta\eta)^2\right]^{1/2} > 0.4 \tag{16}$$

between the lepton and the jets as well as each pair of jets.

To improve the signal/background ratio and to estimate the $H^\pm$ mass we follow a strategy similar to that in [2], except for the step (e) below, which is new.

(a) The invariant mass of two untagged jets is required be consistent with $M_W \pm 15$ GeV.

(b) The neutrino momentum is reconstructed by equating p_ν^T with $\not{p}_T$ and fixing p_ν^L within a quadratic ambiguity via $m(\ell\nu) = M_W$.

(c) The invariant mass of the above untagged jet pair with one of the 3 b-tagged jets is required to be consistent with $m_t \pm 25$ GeV. If several b-tagged jets satisfy this, the one giving the best agreement with m_t is selected.

(d) The invariant mass of the ℓ and ν with one of the 2 remaining b-jets is required to be consistent with $m_t \pm 25$ GeV. In case of several combinations satisfying this, the one giving best agreement with m_t is selected along with the corresponding b-jet and p_ν^L.

(e) The remaining (3rd) b-jet is the one accompanying the $t\bar{t}$ pair in the signal (8) or in the backgrounds (10)–(12)[1]. For the signal it mainly comes from the $H^- \to \bar{t}b$ decay and is therefore quite hard, while it is expected to be very soft for the background processes. Hence the p_T-distribution of this b-jet shall be used to improve the signal/background ratio.

(f) Finally we combine each of the top (anti)quarks in the reconstructed $t\bar{t}$ pair with the 3rd b-jet. Thus we obtain 2 entries per event in the M_{bt} invariant mass plot, one of which would correspond to the $H^\pm$ mass peak for the signal.

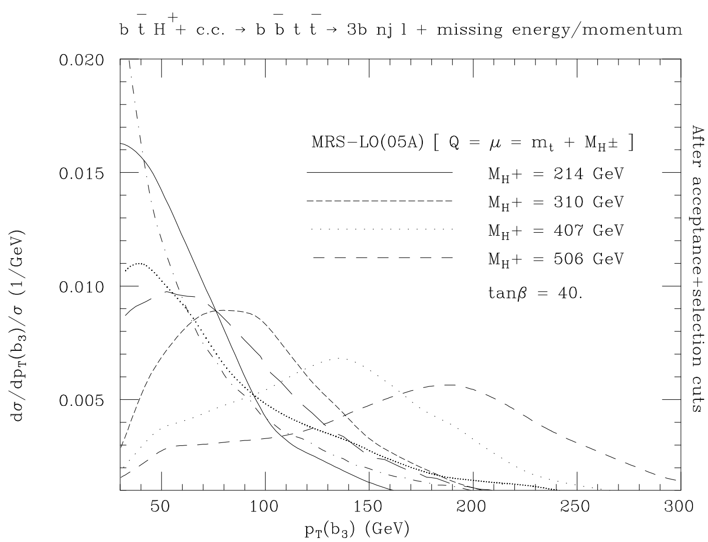

Figure 2: Differential distributions in transverse momentum of the b-quark accompanying the reconstructed $t\bar{t}$ pair in the signal (2)–(3), for four selected values of $M_{H^\pm}$ in the heavy mass range, with $\tan\beta = 40$, after the acceptance and selection cuts described in the text: i.e. eqs. (15)–(16) and steps (a)–(d). The PDF set used was MRS-LO(05A) with renormalisation and factorisation scales set equal to $m_t + M_{H^\pm}$. The (fine-dotted)[long-dashed]{dot-dashed} curve represents the shape of the background process ((10))[(11)]{(12)}. Normalisation is to unity.

Fig. 2 shows the p_T distribution of the 3rd b-jet accompanying the reconstructed $t\bar{t}$ pair as discussed above in step (e). We clearly see a harder p_T distribution for the signal compared to the background processes for a $H^\pm$ mass ≥ 300 GeV. Thus we can improve the signal/background ratio over this mass range by imposing a

$$p_T > 80 \text{ GeV} \tag{17}$$

cut on this 3rd b-jet.

The top of Fig. 3 shows the signal cross-section along with those of the background processes (10)–(12) after applying the selection cuts (15)–(16) and the mass constraints of

[1]In case of a 4th b-jet surviving the $p_T > 30$ GeV cut the harder of the two b-jets accompanying the $t\bar{t}$ pair is selected.

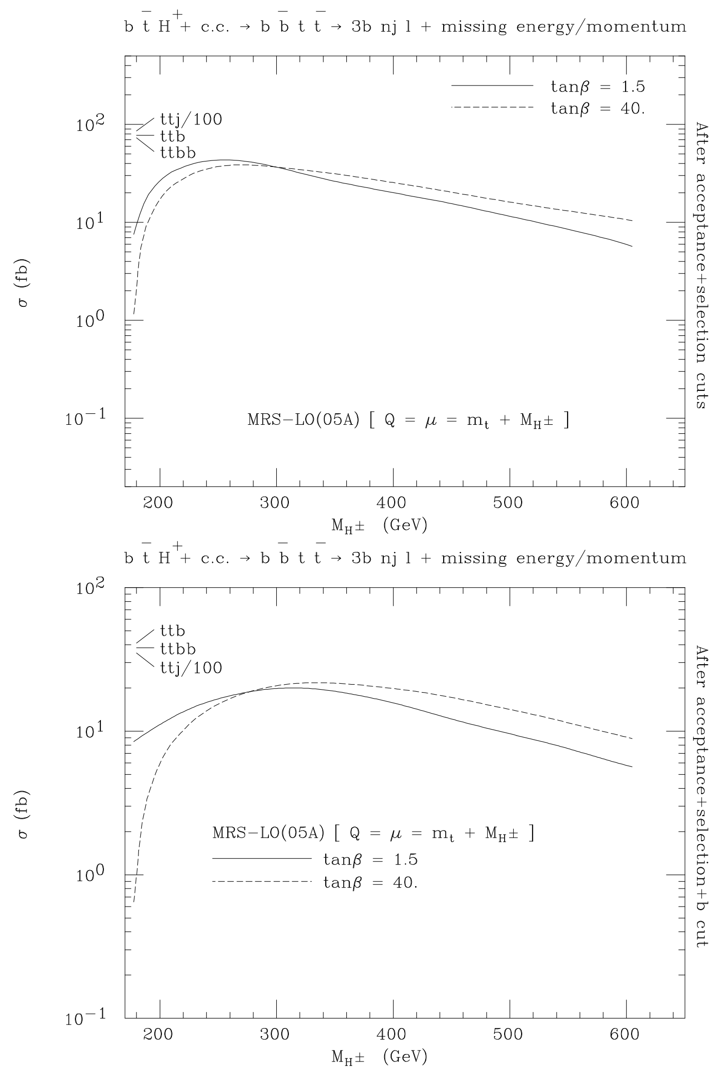

Figure 3: Production cross section for the signal (2)–(3) as a function of $M_{H^\pm}$ in the heavy mass range, after the acceptance and selection cuts described in the text: i.e. eqs. (15)–(16) and steps (a)–(d) (top plot) as well as the transverse momentum cut (17) on the b-jet accompanying the top-antitop pair (bottom plot). The PDF set used was MRS-LO(05A) with renormalisation and factorisation scales set equal to $m_t + M_{H^\pm}$. The arrows represent the size of the backgrounds (10)–(12), the last of which has been divided by 100 (for readability). No b-tagging efficiency/rejection is included.

steps (a)–(d). No b-tagging efficiency or rejection factor has been applied yet. The effect of imposing the p_T-cut (17) on the 3rd b-jet is presented in the bottom plot. It is clearly shown to suppress the backgrounds significantly: in particular the dominant one from ttj (12) is reduced by a factor of 2.5 or so. In contrast the signal cross-section is essentially unaffected for a $H^\pm$ mass ≥ 400 GeV.

Finally, Fig. 4 shows the signal and background cross-sections against the reconstructed

bt invariant mass as discussed in step (f). Here we have included a b-tagging efficiency of 40% and a probability of 1% for mis-tagging a light quark or gluon jet (j) as b-jet [11]. The top figure shows the signal and background cross-sections separately while the bottom one shows their sum for different $H^{\pm}$ masses at $\tan\beta = 40$. The signal peaks are clearly visible in the latter. One gets similar results for $\tan\beta = 1.5$.

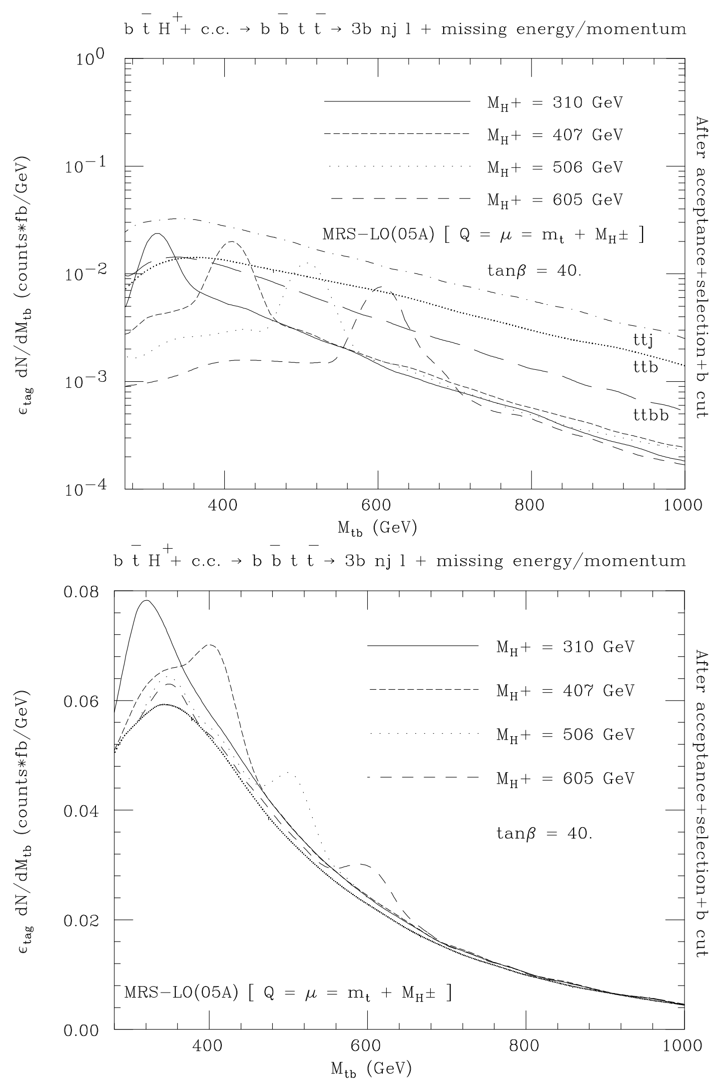

Figure 4: (Top plot) Differential distribution (two entries per each event generated) in the reconstructed charged Higgs mass for the signal (2)–(3), corresponding to four selected values of $M_{H^{\pm}}$ in the heavy mass range, for $\tan\beta = 40$, after the acceptance and selection cuts described in the text: i.e. eqs. (15)–(16) and steps (a)–(d) as well as the transverse momentum cut (17) on the b-jet accompanying the top-antitop pair. The PDF set used was MRS-LO(05A) with renormalisation and factorisation scales set equal to $m_t + M_{H^{\pm}}$. The (fine-dotted)[long-dashed]{dot-dashed} curve represents the shape of the background process ((10))[(11)]{(12)}. (Bottom plot) As above, after summing each signal to all backgrounds. Tagging efficiencies have been included here, in both plots.

Tab. 1 lists the number of signal and background events over a 80 GeV bin around the $H^{\pm}$ mass for an annual luminosity of 100 fb^{-1}, expected from the high luminosity run of the LHC. The corresponding values of $S/\sqrt{B}$ are also shown. We see a better than $5(3)\sigma$ signal up to a $H^{\pm}$ mass of 400(600) GeV at $\tan\beta = 40$. It may be noted that both the signal size and the $S/\sqrt{B}$ ratio are better here in comparison with the 4 b-tagged channel [4] for $\epsilon_b = 40\%$ and p_T cut of 30 GeV. But the S/B ratio is better in the latter case. Similar results hold for $\tan\beta = 1.5$.

Number of events per year			
$M_{H^\pm} \pm 40$ GeV	S	B	$S/\sqrt{B}$
310	133	443	6.2
407	111	403	5.6
506	73	266	4.5
605	43	156	3.4
MRS-LO [$Q = \mu = m_t + M_{H^\pm}$]			
$3b$ + n jets + $\ell^{\pm}$ + $p^T_{\rm miss}$ (with $n = 2, 3$)			After all cuts

Table 1: Number of events from the signal (2)–(3), S, and the sum of the backgrounds (10)–(12), B, along with the statistical significance, $S/\sqrt{B}$, per 100 inverse femtobarns of integrated luminosity, in a window of 80 GeV around four selected values of $M_{H^\pm}$ (given in GeV) in the heavy mass range, for $\tan\beta = 40$. At least three b-jets are assumed to be tagged, each with efficiency $\epsilon_b = 40\%$, whereas the rejection factor against light jets is $\epsilon_{j=q,g} = 1\%$. All cuts discussed in the text, i.e. eqs. (15)–(16), steps (a)–(d) as well as the transverse momentum cut (17) on the b-jet accompanying the top-antitop pair, have been enforced. The PDF set used was MRS-LO(05A) with renormalisation and factorisation scales set equal to $m_t + M_{H^\pm}$.

In summary, the isolated lepton + multi-jet channel with triple b-tagging – supplemented by a transverse momentum cut on the third b-jet – offers a promising signature for $H^{\pm}$ searches at the LHC up to $M_{H^\pm} \approx 600$ GeV at $\tan\beta \gtrsim 40$ and $\lesssim 1.5$, thus extending the reach of previous similar analyses [2,3]. Hence it calls for a more detailed study, including hadronisation, jet identification and detector effects.

Acknowledgements: This work was started at the Les Houches Workshop on Physics at TeV Colliders, organised by LAPP, Annecy. We thank the organisers, Patrick Aurenche and Fawzi Boudjema, for a very stimulating environment. The work of DPR was partly supported by the IFCPAR under project No. 1701-1. SM acknowledges financial support from the UK-PPARC.

References

[1] J.F. Gunion, H.E. Haber, G.L. Kane and S. Dawson, "The Higgs Hunters' Guide" (Addison-Wesley, Reading, MA, 1990).

[2] V. Barger, R.J.N. Phillips and D.P. Roy, Phys. Lett. B324 (1994) 236.

[3] J.F. Gunion, Phys. Lett. B322 (1994) 125.

[4] D.J. Miller, S. Moretti, D.P. Roy and W.J. Stirling, hep-ph/9906230.

[5] K. Odagiri, hep-ph/9901432; D.P. Roy, Phys. Lett. B459 (1999) 607.

[6] A.A. Barrientos Bendezú and B.A. Kniehl, Phys. Rev. D59 (1999) 015009; S. Moretti and K. Odagiri, Phys. Rev. D59 (1999) 055008.

[7] A.A. Barrientos Bendezú and B.A. Kniehl, hep-ph/9908385.

[8] M. Drees, M. Guchait and D.P. Roy, hep-ph/9909266; S. Moretti and K. Odagiri, in preparation.

[9] F. Borzumati, J.-L. Kneur and N. Polonsky, hep-ph/9905443.

[10] D. Dicus, T. Stelzer, Z. Sullivan and S. Willenbrock, Phys. Rev. D59 (1999) 094016.

[11] E. Richter-Was and M. Sapinski, ATLAS note (ATL-PHYS-98-132); V. Drollinger, T. Mueller and R. Kinnunen, CMS note (1999/001).

[12] A.D. Martin, R.G. Roberts, W.J. Stirling and R.S. Thorne, Phys. Lett. B443 (1998) 301.

[13] H.L. Lai et al., Phys. Rev. D55 (1997) 1280.

[14] R. Barnett, H. Haber and D. Soper, Nucl. Phys. B306 (1988) 697; F. Olness and W.K. Tung, Nucl. Phys. B308 (1988) 813; M. Aivazis, J. Collins, F. Olness and W.-K. Tung, Phys. Rev. D50 (1994) 3085; Phys. Rev. D50 (1994) 3102.

[15] A.D. Martin, R.G. Roberts, M.G. Ryskin and W.J. Stirling, Eur. Phys. J. C2 (1998) 287; H.L. Lai and W.K. Tung, Z. Phys. C74 (1997) 463; M. Buza, Y. Matiounine, J. Smith and W.L. van Neerven, Eur. Phys. J. C1 (1998) 301; Phys. Lett. B411 (1997) 211.

[16] L.G. Jin, C.S. Li, R.J. Oakes and S.H. Zhu, hep-ph/9907482.

[17] J.A. Coarasa, D. Garcia, J. Guasch, R.A. Jiménez and J. Solà, Eur. Phys. J. C2 (1998) 373.

[18] T. Stelzer and W.F. Long, Comp. Phys. Comm. 81, 357 (1994).

[19] H. Murayama, I. Watanabe and K. Hagiwara, HELAS: HELicity Amplitude Subroutines for Feynman Diagram Evaluations, *KEK Report* 91-11, January 1992.